Biophysical Chemistry 21 (1985) 103–114
Elsevier

BPC 00896

SELF-ASSOCIATION OF SODIUM CHOLATE IN ISOTONIC SALINE SOLUTIONS

John M. BECKERDITE * and E.T. ADAMS, Jr **

Chemistry Department, Texas A&M University, College Station, TX 77843, U.S.A.

Received 27th April 1984
Accepted 26th July 1984

Key words: Self-association; Sodium cholate; Vapor pressure osmometry; Sedimentation equilibrium; Osmotic coefficient; Apparent weight average molecular weight

The self-association of dialyzed solutions of sodium cholate in isotonic saline solutions has been studied by vapor pressure osmometry and sedimentation equilibrium. These studies were carried out at 25, 31 and 37°C. In all experiments the self-association could be described as a two-equilibrium constant, indefinite self-association in which odd species beyond monomer were absent. The plots of M_1/M_{na} or M_1/M_{wa} vs. c were quite smooth with no sharp breaks; this suggested that there were no critical phenomena. The temperature dependence of the self-association was quite small. Our results are in accord with other studies on sodium cholate which indicate that the self-association involves several species, and that it is not a monomer-n-mer self-association.

1. Introduction

Many biologically important molecules are known to undergo self-association in solution. Of particular interest are the bile salts, whose mode of self-association is not well known. These biologically important surfactants are found in the bile, and are involved in the emulsification and absorption of fats and oils [1–7]. Their ability to do so is in some way related to their unique structure which, with the exception of the sodium salts of ursodeoxycholic acid and its glycine and taurine conjugates, has the hydrophilic hydroxyl groups on one side of the steroid backbone and the hydrophobic groups on the other side [2,3,7]. Under physiological conditions bile salts undergo self-association, but the extent of association varies with the bile salt and also with the solution conditions [2–4,6–8]. Sodium cholate, which we report on here, is initially synthesized from cholesterol in the liver in the form of a free acid [1–3]; even though synthesized as an acid, under physiological conditions it is present as the completely dissociated salt. Sodium cholate is referred to as a primary bile salt. Like all bile salts it may be conjugated with glycine or taurine [2,3]. Fig. 1 shows the structure of cholic acid; the three hydroxyl groups are all on the same side of the steroid backbone at the 3α, 7α and 12α positions.

In solution bile salts self-associate strongly, pre-

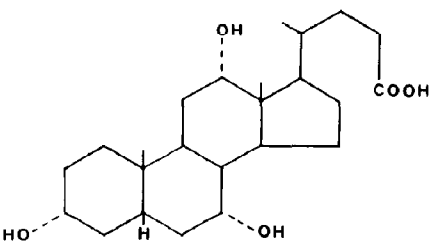

Fig. 1. Structure of cholic acid. Note that the three hydroxyl groups at carbons 3, 7 and 12 are all in the α position.

* This paper is taken from the dissertation submitted by John M. Beckerdite in partial fulfillment of the requirements of Graduate College, Texas A&M University for the degree of Doctor of Philosophy (August 1983).

** To whom correspondence should be addressed.

sumably via intermolecular hydrogen bonding or a hydrophobic interaction; which interaction occurs has been the subject of controversy. Infrared and ultraviolet absorbances, as well as NMR, were used by Bennet et al. [9] to reveal unusually persistent intermolecular hydrogen bonding in several bile acids. Oakenfull and Fisher [10], on the basis of conductance and density studies in water/ethanol solutions, claim that at low concentrations self-associations are generated through polyfunctional hydrogen bonding of the bile salt hydroxyl groups. This is disputed by Zana [11] who challenged their measurements and argues in favor of a hydrophobic interaction theory. The hydrophobic interaction theory was first made popular by Small [8,12]; he postulated the formation of 'primary' micelles held together by hydrophobic forces, which under certain conditions could join each other through intermolecular hydrogen bonding to form even larger 'secondary' micelles. Mazer et al. [7], who used quasielastic light scattering to study the self-association of several bile salts, also felt that the association proceeds in two stages. In their scheme the first stage is a hydrophobic association of bile salt monomers into small primary micelles, which at higher concentrations undergo additional hydrophobic associations into larger secondary micelles. Vadnere and Lindenbaum [6], who studied the self-association of bile salts by obtaining partition coefficients of bile salts in a two phase system (1-octanol and aqueous buffer solutions), felt that their results were consistent with hydrophobic interaction occurring first followed by hydrogen bonding interactions.

The greatest controversy, however, deals with the nature of the distribution and size of the associated complexes. Ekwall [13–17] reported sudden increases in the solubility of lipophiles in bile salt solutions as the bile salt concentrations increased; he designated these limits as 1, 2 and 3. Studies by Fontell [18–20] concluded that no self-association took place below limit 1, and that it increased gradually beyond this point. These limits became associated with the concept of a critical micelle concentration (CMC). Carey and Small [21] claim evidence for CMCs on the basis of maximum absorption of rhodamine 6G in solutions of bile salts. Kratohvil and DelliColli [22] gave CMC values based on surface tension and light scattering; they have also reported on the aggregation of sodium taurodeoxycholate under various solution conditions, assuming a monomer-n-mer association model [23]. Small [3] has presented an extensive compilation of CMC determinations by various methods; he points out that each method may give somewhat different values for the CMC. On the other hand, studies by Mazer et al. [7] using quasielastic light scattering, elastic light scattering experiments by Chang and Cardinal [4], and partition coefficient measurements by Vadnere and Lindenbaum [6] indicate that the self-association of bile salts is not a simple monomer-n-mer association, but involves several self-associating species.

Since we have had experience in our laboratory studying self-associations under ideal or nonideal solution conditions, we felt that the self-association of bile salts needed to be studied. We have developed a number of models to test for what type of self-association is present, and once a model has been chosen we can evaluate the equilibrium constant (k_i) or constants and the nonideal term (BM_1). Most work on bile salt self-associations has been done assuming ideal solution conditions; however, Chang and Cardinal [4] did attempt to correct their light scattering data for nonideal behavior, and Mazer et al. [7] did consider electrostatic and solvent-micelle interactions. Here we report on sedimentation equilibrium experiments at 25°C and on vapor pressure osmometry experiments at 31 and 37°C on solutions of sodium cholate, which have been dialyzed against isotonic saline (0.154 M NaCl). While the ultracentrifuge can be used at temperatures higher than 30°C, provided that it has been modified with a high-temperature unit, one cannot use an unmodified ultracentrifuge above 30°C since oil from the drive condenses on the schlieren lenses. Since we wanted to see how bile salts self-associate at body temperature (37°C) in order to mimic physiological conditions, we used vapor pressure osmometry. It will be seen that the results from the two experimental techniques are in accord with each other.

2. Experimental

2.1. Preparation of sodium cholate solutions

The chemicals used in the sedimentation equilibrium and vapor pressure osmometry (VPO) experiments were of the highest grade commercially available. Sodium cholate was obtained from Sigma Chemical Co. (grade I, > 99% purity). Thin-layer chromatography (TLC) was used as a check on the purity. The TLC plate was run using a trimethylpentane/ethyl acetate/water (5 : 5 : 1, v/v) solvent system and was developed by spraying with concentrated H_2SO_4; only one spot occurred with an R_f value corresponding to that reported by Eneroth [24].

Dialysis of the sodium cholate was accomplished with the use of a Bio-Rad cellulose acetate hollow fiber dialyzer with a 200 g/mol molecular weight cut-off. The monomer molecular weight of sodium cholate is $M_1 = 430.54$ g/mol. The bile salt solutions to be dialyzed were made up according to ideal Donnan equilibrium conditions using NaCl as the supporting electrolyte. For the dialysis, the solution to be dialyzed was placed on the outside of the fibers, and the dialysate (0.154 M NaCl) was run through the inside of the hollow fibers, which were in contact with sodium cholate solution. A source tank containing 20 l of dialysate was connected to the input port, and another tube connected to the outlet port carried the dialysate to the collection tank. Prior conductivity measurements showed that 10 cycles of the 20 l of dialysate through the fibers were more than sufficient to achieve dialysis equilibrium. A magnetic stirrer was used to mix the outer sodium cholate solution; dialysis was carried out in the cold room (4–6°C). The isotonic saline (0.154 M NaCl) dialysate was prepared from reagent grade NaCl and from water redistilled from an all-glass still.

The concentrations of the dialyzed bile salt solutions were determined spectrophotometrically at 388 nm using a procedure similar to that used by Gänshirt et al. [25]. Here 10 ml each of several solutions of known concentrations of bile salts were pipetted into 25-ml flasks; these flasks were then placed in an ice bath and allowed to equilibrate. Then, 10 ml of fresh, reagent grade H_2SO_4 were added slowly over a period of about 3 min. During this time that the acid was being added, the flask was kept immersed in an ice bath and a constant swirling motion was applied. The solutions were then heated in stoppered flasks at 60°C for 4 h. With sodium cholate, a trihydroxy bile salt, two distinct maxima were observed at 320 and 388 nm; a linear Beer-Lambert plot was obtained based on the absorbance at 388 nm. Good linearity was obtained up to an absorbance of 0.5; the extinction coefficient was 32.7 ± 0.2 l g^{-1} cm^{-1} at 388 nm.

2.2. Vapor pressure osmometry (VPO) experiments

The Knauer vapor pressure osmometer was used; in general, previously described procedures were followed [26–28]. The temperatures used were 31 and 37°C. The bridge was calibrated on scale A to give a full scale deflection (on a 10 inch chart recorder) at 200 μV imblance. Reagent grade sucrose was used as the standard. The syringes used to introduce the sample to the thermistor probes were warmed up in the VPO for 5 min before the drops were added to the probes. Each probe was rinsed with four drops of dialysate or solution before the measures were made. 10 min were generally sufficient to obtain a stable baseline of dialysate vs. dialysate. A steady-state temperature change was usually observed when solution and dialysate were used. The chart recorder deflections were extrapolated back to the time of injection, and the vertical difference between this point and the baseline was used to obtain the ΔE (microvolts imbalance) value for this concentration.

2.3. Sedimentation equilibrium experiments

Sedimentation equilibrium experiments were performed as described previously [29–31] on a Beckman model E analytical ultracentrifuge at 25°C and at 32 000 rpm. For these experiments an He-Ne modulatable laser was used as the light source (λ = 632.8 nm). A black, four-hole, aluminum alloy (AN-K) rotor was used, so that three experiments could be performed at the same time. Carbon-filled epoxy, double-sector centerpieces were used; no layering oil was used. In

order to prevent interchannel communication across the central rib, a special circular polyethylene gasket with a central rib was placed between the sapphire windows and the centerpiece. It was found by experience that the edges of the gaskets opposite the filling holes had to be trimmed to allow an unobstructed light path along the cell bottom. Slightly longer columns (≈ 6 mm) were used, and the times to reach equilibrium were estimated from the equation of Van Holde and Baldwin [32]. At least 8 h were added to this calculated time as a precautionary measure.

The density of the solvent (ρ_0), the density increment at constant temperature and chemical potential ($1000(\partial\rho/\partial c)_{T,\mu}$) and the apparent specific volume (ϕ') of sodium cholate were obtained from measurements on a digital precision density meter (Anton Paar Model DMA-02C) at 20°C. The calibration constant was based on the densities of water and air (corrected for relative humidity). Solution densities were corrected to 25°C by assuming $(\rho_{25}/\rho_{20})_{\text{solution}} = (\rho_{25}/\rho_{20})_{H_2O}$. At 25°C for 0.154 M NaCl $\rho_0 = 1.00351$ g/cm^3. Fig. 2 shows a plot of the solution density (ρ) vs. solute concentration (c) in g/l; the density increment is obtained from the slope of this plot. At 25°C the density increment was $1000\ (\partial\rho/\partial c)_{T,\mu} = 0.206 \pm 0.003$, and the apparent specific volume was $\phi' = 0.791 \pm 0.003$ cm^3/g.

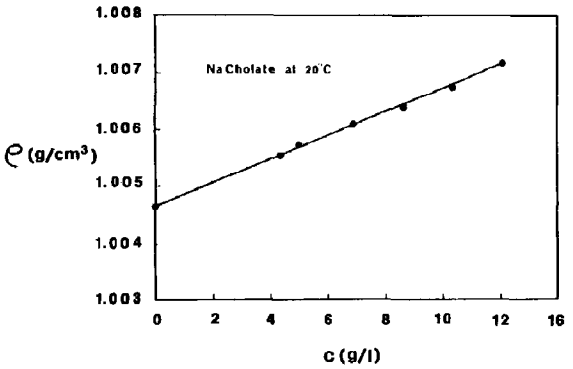

Fig. 2. Plot of ρ vs. c for dialyzed sodium cholate solutions at 20°C. The density increment is obtained from the slope of this plot since for c in g/l

$$\rho = \rho_0 + 1000(\partial\rho/\partial c)_{T,\mu}(c/1000)$$
$$= \rho_0 + (1 - \phi'\rho_0)(c/1000)$$

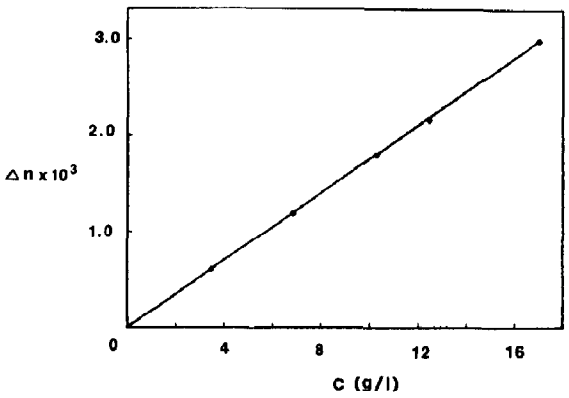

Fig. 3. Plot of Δn vs. c for dialyzed sodium cholate solutions at 25°C and $\lambda = 546$ nm. The refractive index increment ψ is obtained from the slope of this plot.

The concentration units obtained from the Rayleigh interferometric optical system in the ultracentrifuge are in fringes, J, and are related to $\Delta n = n - n_0$, the refractive index difference between solution (n) and solvent (n_0) or dialysate, by

$$J = (\Delta n)h/\lambda \tag{1}$$

where h is the centerpiece thickness (12 mm) and λ (632.8 nm) is the wavelength of light used. Δn is related to the concentration c (in g/l) by the refractive index increment at constant temperature and chemical potential, ψ. Thus

$$\Delta n = \psi c \tag{2}$$

and J is related to c by

$$J = h\psi c/\lambda \tag{3}$$

The refractive index difference, Δn, was measured at 25°C with a Brice-Phoenix Model BP-2000 V differential refractometer, using a wavelength of 546 nm; these values were converted to Δn at 632.8 nm as described previously [31,33]. KCl solutions were used to calibrate the differential refractometer.

In order to determine the refractive index increment, ψ, various dialyzed solutions of sodium cholate were made up, and from a plot of Δn vs. c (see fig. 3), ψ was obtained as the slope. This plot was linear. Sodium cholate concentractions were

determined spectrophotometrically as described earlier. We were able to show using sodium cholate solutions with different NaCl concentrations, that there was no effect of the salt on the absorbance of sodium cholate at 388. The values of the refractive index increment were $\psi = (1.742 \pm 0.005) \times 10^{-4}$ l/g at 546 nm and $\psi = (1.739 \pm 0.005) \times 10^{-4}$ l/g at 632.8 nm.

3. Results

3.1. Quantities needed for the analysis

First of all, it is assumed that previously used assumptions [26–31] apply: (1) The natural logarithm of the activity coefficient ($\ln y_i$) of any self-associating species can be described by

$$\ln y_i = iB_* M_1 c, \qquad i = 1, 2, \ldots \tag{4}$$

where B_* is a constant, whose value depends on the self-associating solute and the solution conditions, $M_1 = 430.54$ g/mol (for sodium cholate) is the monomer molecular weight, and c is the total solute concentration in g/l. (2) The partial specific volumes ($\bar{v}$) or the density increments $(1000(\partial\rho/\partial c)_{T,\mu})$ are the same for each self-associating species. (3) The refractive index increments are the same. The first assumption applies to both techniques. Assumptions 2 and 3 apply to sedimentation equilibrium experiments; these assumptions are not needed for vapour pressure osmometry experiments.

When the first assumption applies, then $y_n/y_1^n = 1$ and the total solute concentration becomes

$$c = c_1 + c_2 + c_3 + \ldots \tag{5}$$
$$= c_1 + k_2 c_1^2 + k_3 c_1^3 + \ldots$$

where

$$c_n = k_n c_1^n \qquad (n = 2, 3, \ldots) \tag{6}$$

From VPO experiments one can obtain M_{na}, M_{wa} and $\ln f_a$. These quantities can be used to test for the type of equilibrium present and to evaluate the equilibrium constant(s), k_i, and the nonideal term, BM_1. The apparent number average molecular weight, M_{na}, is obtained from [26–28]

$$\Delta E = K_{VP}(c/M_{na}) \tag{7}$$

where K_{VP} is the instrument calibration constant, whose value depends mainly on the solvent and the temperature. K_{VP} is evaluated from a calibration experiment at the same temperature and in the same solvent using a nonvolatile solute of known molecule weight; here sucrose was used. M_{na} is related to the true number average molecular weight, M_{nc}. by [26–28]

$$\frac{M_1}{M_{na}} = \frac{M_1}{M_{nc}} + \frac{BM_1 c}{2} \tag{8}$$

Here

$$B = B_* + (\bar{v}/1000M_1) \tag{9}$$

and

$$M_{nc} = c/\Sigma(c_i/M_i) \tag{10}$$

The apparent weight average molecular weight, M_{wa}, is related to M_{na} for self-associations by the equation [26–28]

$$\frac{M_1}{M_{wa}} = \frac{M_1}{M_{na}} + c\frac{\mathrm{d}}{\mathrm{d}c}\left(\frac{M_1}{M_{na}}\right) \tag{11}$$

and M_{wa} is related to the ideal weight average molecular weight by

$$\frac{M_1}{M_{wa}} = \frac{M_1}{M_{wc}} + BM_1 c \tag{12}$$

M_{wc} is defined by

$$M_{wc} = (\Sigma c_i M_i)/c$$
$$= M_1 \Sigma(ic_i)/c \tag{13}$$

since $M_i = iM_1$ $(i = 2, 3, \ldots)$. Similarly, one can obtain the natural logarithm of the weight fraction of monomer, $\ln f_1$, or its apparent value, $\ln f_a$, under nonideal conditions from [26–28]

$$\ln f_a = \int_0^c \left(\frac{M_1}{M_{na}} - 1\right)\frac{\mathrm{d}c}{c} + \left(\frac{M_1}{M_{na}} - 1\right) \tag{14}$$

Here

$$\ln f_a = \ln f_1 + BM_1 c \tag{15}$$

and

$$f_1 = c_1/c \tag{16}$$

For an ideal solution $BM_1 = 0$, and M_{na}, M_{wa} and $\ln f_a$ have their ideal values.

From sedimentation equilibrium experiments one obtains the following relations [29–31,33]:

$$M_{wa} = \frac{1}{A} \cdot \frac{d\ln c}{d(r^2)} \tag{17}$$

$$M_{na} = \frac{1}{c}\int_0^c \frac{M_1}{M_{wa}} dc \tag{18}$$

and

$$\ln f_a = \int_0^c \left(\frac{M_1}{M_{wa}} - 1 \right) \frac{dc}{c} \tag{19}$$

Here

$$A = 1000(\partial\rho/\partial c)_{T,\mu}\omega^2/2RT \tag{20}$$

and M_{wa} is defined by eq. 12. In these equations c refers to the total solute concentration at any radial position r (from the center of rotation) in the solution column of the ultracentrifuge cell between r_m, the air/solution meniscus, and r_b, the radial position of the cell bottom. R is the universal gas constant (8.314×10^7 erg K^{-1} mol^{-1}), T the absolute temperature, $\omega = 2\pi(\text{rpm})/60$ the angular velocity of the rotor and $1000(\partial\rho/\partial c)_{T,\mu}$ the density increment.

One can use combinations of M_{wa}, M_{na} and $\ln f_a$ (which can be obtained from either vapor pressure osmometry or sedimentation equilibrium experiments) to analyze self-associations. Two useful functions are [26–31,33]

$$\eta = \frac{M_1}{M_{wa}} - \ln f_a = \frac{M_1}{M_{wc}} - \ln f_1 \tag{21}$$

and

$$\xi = \frac{2M_1}{M_{na}} - \frac{M_1}{M_{wa}} = \frac{2M_1}{M_{nc}} - \frac{M_1}{M_{wc}} \tag{22}$$

Note that the nonideal term BM_1 has been eliminated in the expressions for η and ξ; also note that values of these quantities are independent of any model. We can use these quantities to analyze various self-associations; the details for doing this are described extensively elsewhere [26–31,34–36].

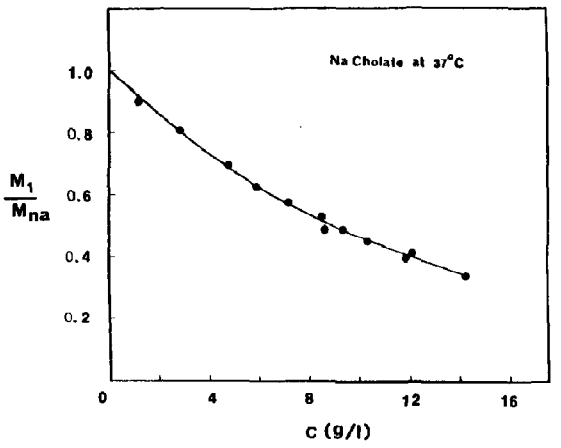

Fig. 4. Vapor pressure osmometry. Plot of M_1/M_{na} (the osmotic coefficient) vs. c at 37°C for dialyzed sodium cholate solutions. Note the continuous decrease in M_1/M_{na} with increasing c, which is characteristic of some self-associations.

3.2. *Vapor pressure osmometry results*

Figs. 4 and 5 show plots of the osmotic coefficient, M_1/M_{na} vs. c at 37 and 31°C, respectively, for sodium cholate dialyzed against isotonic saline. The decrease in M_1/M_{na} with increasing c is characteristic of self-associations. The data at 31 and 37°C were smoothed and used to obtain M_{na},

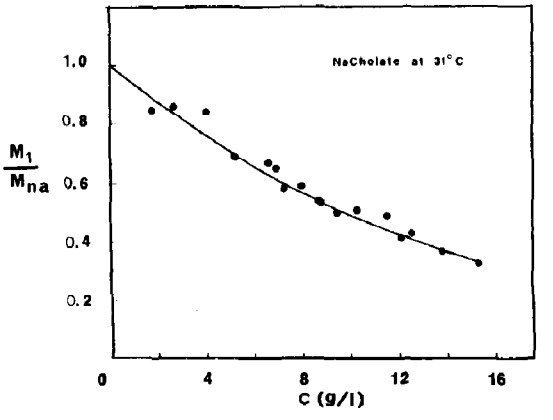

Fig. 5. Vapor pressure osmometry. Plot of M_1/M_{na} vs. c at 31°C for dialyzed sodium cholate solutions.

Table 1

Equilibrium constants and nonideal term for the type IV SEK indefinite self-association of sodium cholate in isotonic saline

T (°C)	k_{12} ($l\,g^{-1}$)	k ($l\,g^{-1}$)	BM_1 ($l\,g^{-1}$)	Variance [a]	K_{12} [b] (M^{-1})	K [c] (M^{-1})
25	0.063 ± 0.001	0.62 ± 0.01	0.0003 ± 0.0002	2.07×10^{-4}	27.1 ± 0.4	$(2.67 \pm 0.04) \times 10^2$
31	0.059 ± 0.002	0.50 ± 0.02	-0.0143 ± 0.0002	1.89×10^{-5}	25.4 ± 0.9	$(2.15 \pm 0.09) \times 10^2$
37	0.081 ± 0.001	0.46 ± 0.01	-0.0133 ± 0.0001	4.98×10^{-6}	34.8 ± 0.4	$(1.98 \pm 0.04) \times 10^2$

[a] Variance $= \frac{1}{N-p} \cdot \sum_{i=1}^{N} \delta_i^2$, where N is the number of data points used, p the number of parameters (3 for the type IV SEK model) and $\delta_i = [(M_1/M_{na})_{obsd} - (M_1/M_{na})_{calcd}]_i$ or $[(M_1/M_{wa})_{obsd} - (M_1/M_{wa})_{calcd}]_i$.

[b] $K_{12} = k_{12} M_1$. Here $M_1 = 430.54$ g/mol.

[c] $K = kM_1$.

M_{wa}, $\ln f_a$, η and ξ from eqs. 7, 11, 14, 21 and 22. The next step was to test for the type of self-association that was present. Various monomer-n-mer associations (up to $n = 20$) were tried with the 37°C data. These models failed, with the fit becoming worse as the value of n was increased. Neither were we able to find a monomer-n-mer-j-mer (monomer-dimer-trimer, etc.) model to describe the self-association. Finally, we tried eight indefinite self-associations – four AK (attenuated equilibrium constant) and four SEK (sequential, equal equilibrium constant) models. None of the AK models worked. Only the type IV SEK model gave a good description of the data. The 31°C data were subjected to the same analysis, and these data also were best described by the type IV SEK model. Figs. 4 and 5 show the regenerated fit (solid line) based on the recovered equilibrium constants and nonideal terms for these data. Table 1 shows values of k_{12} (the dimerization constant), k (the stepwise association constant) and BM_1 (the nonideal term) for this model. For more details about this self-association consult the appendix.

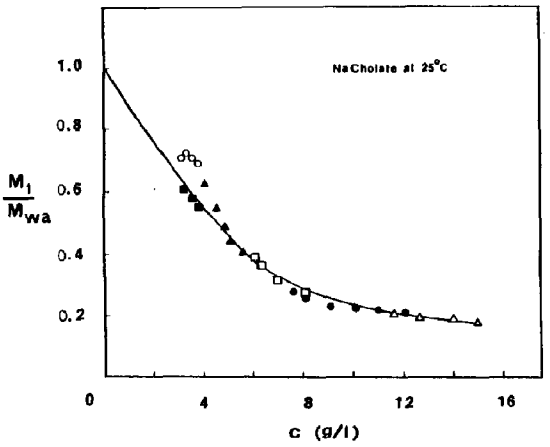

Fig. 6. Sedimentation equilibrium. Plot of M_1/M_{wa} vs. c at 25°C for dialyzed sodium cholate solutions. The continuous decrease in M_1/M_{wa} with increasing c indicates the presence of a self-association.

3.3. Sedimentation equilibrium results

Values of M_{wa} were obtained from eq. 17. Fig. 6 shows plots of M_1/M_{wa} vs. c at 25°C for sodium cholate dialyzed against 0.154 M NaCl. The different symbols indicate solutions having different initial concentrations. The decrease in M_1/M_{wa} with increasing c is characteristic of self-associations. These data were smoothed, and values of M_{na}, $\ln f_a$, η and ξ were calculated from eqs. 18, 19, 21 and 22. Note that the self-association appears to be fairly strong, going to M_1/M_{wa} values close to 0.2 at $c = 15$ g/l. We tried the various models for self-association described above for the VPO experiments, and a type IV SEK model seemed to give the best description of the data. The solid line in fig. 6 represents the regenerated data. Values of k_{12}, k and BM_1 are listed in table 1.

3.4. Thermodynamic functions

The values of the molar equilibrium constants (K_{12} and K) for the type IV SEK model were obtained from the relations

$$K_{12} = k_{12} M_1 \tag{23}$$

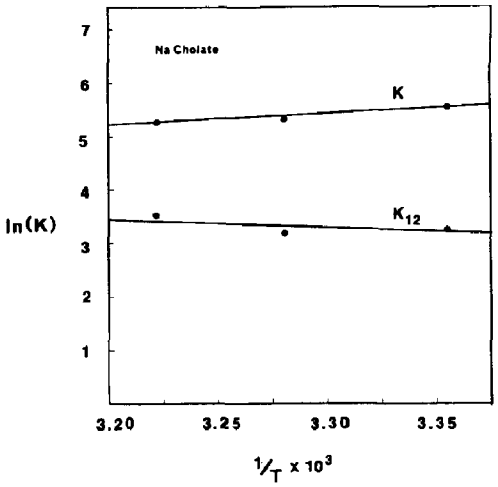

Fig. 7. Van't Hoff plots of ln K_{12} vs. $1/T$ (lower plot) and ln K vs. $1/T$ (upper plot). From the slopes of these plots one obtains $-\Delta H^\circ_{12}/R$ and $-\Delta H^\circ/R$, respectively.

and

$$K = kM_1 \tag{24}$$

We have listed the values of K_{12} and K in table 1. The standard Gibbs free energy change, ΔG°, was obtained from

$$\Delta G_i^\circ = -RT \ln K_i \tag{25}$$

where K_i is K_{12} or K. The change in the standard enthalpy, ΔH°, is obtained from the well known van't Hoff equation

$$(\partial \ln K_i/\partial T)_P = -\Delta H_i^\circ/RT^2 \tag{26}$$

Table 2

Thermodynamic parameters for the type IV SEK model for the self-association of sodium cholate in isotonic saline solutions

T (°C)	ΔG° (kcal mol^{-1})	ΔH° (kcal mol^{-1})	ΔS° (cal mol^{-1} K^{-1})
(A) The dimerization $2P_1 \leftrightharpoons P_2$			
25	-1.96 ± 0.01	3.8 ± 6.4	19 ± 30
31	-1.95 ± 0.02	3.8 ± 6.4	19 ± 32
37	-2.19 ± 0.02	3.8 ± 6.4	19 ± 33
(B) The stepwise association $P_2 + P_{n-2} \leftrightharpoons P_n$ ($n = 4, 6, 8, \ldots$)			
25	-3.31 ± 0.01	-4.6 ± 6.5	-4.3 ± 6.1
31	-3.25 ± 0.02	-4.6 ± 6.5	-4.4 ± 6.3
37	-3.26 ± 0.01	-4.6 ± 6.5	-4.3 ± 6.1

Fig. 7 shows the plots based on eq. 26. The values of ΔS_i°, the standard entropy change, were obtained from

$$\Delta S_i^\circ = (\Delta H_i^\circ - \Delta G_i^\circ)/T \tag{27}$$

Values of ΔG_i°, ΔH_i° and ΔS_i° are tabulated in table 2.

4. Discussion

It was very gratifying to note that we obtained the same model for the self-association of sodium cholate in isotonic saline solution by both experimental techniques. This supports the Adams and Fujita [26–31,33,37] convention for ln y_i (see eq. 4) and the relationships between M_1/M_{na}, M_1/M_{wa} and ln f_a, since this convention and these relations were used in the analysis. The best model that described these self-associations was a type IV SEK indefinite self-association; this is a two-equilibrium constant model [35,36]. Note that the data for all of the experiments with sodium cholate could be described by a smooth curve; this suggests that there are no critical micelle phenomena. The fact that the self-associations were described as indefinite self-associations does not necessarily imply that there are a vast number of self-associating species present. White and Kilpatrick [38], who studied the self-association of 2-(n-butyl)benzimidazole and also benzotriazole in benzene by cryoscopy, used eight equilibrium constants to describe their self-association. These data were reanalyzed by Tobolsky and Thach [39], who showed that a two-equilibrium constant indefinite self-association (an ideal SEK type III model) could describe the data with the same precision.

The sedimentation equilibrium data seem to fit quite well together in the M_1/M_{wa} vs. c plot. This suggests that the assumptions regarding the equality of the refractive index increments and the density increments are reasonable. Otherwise, there would be pressure effects on the self-association, which would make the data not overlap. Note that a linear plot of ρ vs. c is obtained, which indicates that within the precision of the measurements the density increment is constant and does not depend on c. The observed overlap of the M_1/M_{wa} vs. c

data also suggests that salt redistribution effects, due to changes in NaCl concentration in the ultracentrifuge cell, are not significant. When we previously tried dialysis with a hollow fiber dialyzer in our experiments on the self-association of the disodium salt of adenosine 5′-triphosphate (ATP) [31], we did get a lot more scatter in the data, and this may have been due to incomplete dialysis. Here we did pay close attention to the time required for dialysis equilibrium, and the results indicated that the effort was well spent.

In order to study the self-association of bile salts in isotonic saline by vapor pressure osmometry one must do the experiments with great care. Since all measurements were made against the dialysate, it was important that the chemical potentials of the NaCl in the bile salt solution and the dialysate be the same. This condition is met at dialysis equilibrium.

In vapor pressure osmometry, at a given concentration the temperature difference between the solution and reference thermistors is inversely proportional to M_{na} (see eq. 7). For strong associations, such as those encountered with bile salts, M_{na} can be quite large even at low concentrations. As a result ΔT and ΔE can be quite small. Measurements at the manufacturer's highest recommended sensitivity (scale 128) showed deflections too small to be useful. Fortunately, it was possible to expand this scale 3-fold using the special 'A' setting. At this sensitivity (200 μV full scale on a 10 inch chart recorder) the baseline drift was significant. As a result a new baseline had to be established before each solution measurement. Even on this expanded scale, the maximum voltage never exceeded about one-third full scale. Although the thermistor cell was well thermostatted and insulated, small changes in ambient temperature produced large variations in the baseline. An additional problem was encountered with small fluctuations in line voltage; this resulted in sudden, large changes in the ΔE value. As a consequence, the apparatus was placed in an air-conditioned, windowless room, and most of the data were collected at night when temperature and line voltage fluctuations were at a minimum.

The physiological concentrations of bile salts in human hepatic bile range from 7 to 14 g/l [40]; most of the self-association data fall in this region. As solution concentrations were increased beyond about 15 g/l, the ΔE values passed through a maximum and began to decrease. Analysis was truncated at this maximum, since a calculation of either the ideal M_{wc} or the real M_{wa} (see eq. 11) would yield negative values, and this is physically impossible. It is possible that a more sophisticated treatment will have to be developed to account for the observed nonideality in the region. It may be that at 15 g/l, which is approx. 0.035 M with respect to the bile salt monomer compared to 0.154 M NaCl in the dialysate, the decreasing concentration ratio of NaCl to bile salt introduces complicating factors in the association. With proteins and other macromolecules this is less of a problem, since the molar (or formal) concentration is much, much less than that of the supporting electrolyte.

Since sodium cholate ionizes in aqueous solution, it was important to dialyze the sodium cholate against the supporting electrolyte so that one could redefine the sodium cholate according to the Vrij and Overbeek [41] or the Casassa and Eisenberg [42] conventions. This also reduces the equations to ones formally identical with two-component system equations. Since measurements of ultraviolet absorption spectra of sodium cholate in solutions having different NaCl concentrations gave virtually identical spectra, we believe that we are correct in defining the monomer as sodium cholate ($M_1 = 430.54$ g/mol), instead of sodium cholate − (1/2)NaCl. It should be noted that VPO experiments on aqueous bile salt solutions with no supporting electrolyte have been performed by Fontell [18] and by Carpenter and Lindenbaum [43]; their osmotic coefficient data indicated that the bile salts underwent self-association.

From the thermodynamic calculations in table 2 it is difficult to establish any temperature dependence for the self-association of sodium cholate. It is impossible to determine whether $\Delta H°$ is positive or negative; one can only say that it is relatively small in magnitude. The errors in $\Delta S°$ are correspondingly large. The absence of any significant temperature effects on the self-association of sodium cholate in 0.154 M NaCl is in accord with the studies of Carpenter and Lindenbaum [43],

who measured osmotic and activity coefficients of aqueous sodium cholate solutions (no added NaCl) at 25, 37 and 45°C. Other studies on bile salts covering much larger temperature ranges have generally shown a slight increase in association behavior as the temperature decreases [7,8,21,43]. It should be noted that the nonideal terms we measured were quite small; at 25°C the sodium cholate solution was virtually ideal, since $BM_1 \simeq 0$.

Values of the partial specific volumes [8,44] and the refractive index increments [4,19] at constant supporting electrolyte concentration have been reported by others for sodium cholate solutions. Since our measurements of the refractive index increment (ψ) and the apparent partial specific volume (ϕ') were made at constant chemical potential of the supporting electrolyte, we cannot compare these values directly. On the other hand, we can use our values of $\phi' = 0.791$ cm^3/g, $\rho_0 = 1.00351$ g/cm^3, Small's [8] value of $\bar{v}_2 = 0.75$ cm^3/g and a value of $\bar{v}_3 = 0.302$ cm^3/g for 0.154 M NaCl [48] at 25°C to make an estimate of the preferential interaction parameter ξ, since [45–57]

$$\xi = \frac{(1 - \phi'\rho_0) - (1 - \bar{v}_2\rho_0)}{(1 - \bar{v}_3\rho_0)} \tag{28}$$

Note that ξ is a standard symbol for the preferential interaction parameter; it is not to be confused with ξ defined by eq. 22. We obtained $\xi = -0.06 \pm 0.01$ for the preferential interaction parameter. A negative value for ξ indicates that preferential solvation (hydration) is occurring.

The observation that sodium cholate undergoes a two-equilibrium constant indefinite self-association (a type IV SEK model) is in accord with other studies on sodium cholate self-association. Results from several other recent studies seem to favor a stepwise association process. Zana and co-workers [49] pointed out that their ultrasonic relaxation spectra of sodium cholate and sodium deoxycholate solutions were more indicative of a continuous self-association than a true micellization as is found with classical detergents. They also reported association below the limit of approx. 6 g/l for sodium cholate reported by Ekwall [50] and Fontell [18–20,51]. All of the sodium cholate data collected for the present study showed significant self-association below this limit. No monomer-*n*-mer or monomer-*n*-mer-*j*-mer associations could be found to describe the observed self-association of sodium cholate, although monomer-*n*-mer associations seem to describe the self-association of some soaps and detergents [52–55]. This observation is not surprising in view of the differences in chemical structure between a bile salt and a detergent like sodium dodecyl sulfate or a soap like sodium palmitate. Using elastic light scattering, Chang and Cardinal [4] found that the self-association of sodium cholate in various concentrations of NaCl (0.10, 0.30 and 0.50 M) could be interpreted as a monomer-dimer-trimer-aggregate model. Similar results were found with other bile salts [4]. Vadnere and Lindenbaum [6], who studied the partition of sodium cholate between 1-octanol and aqueous buffer solutions (0.02 M tromethamine, pH 8) between 25 and 55°C, interpreted their data as a monomer-dimer-tetramer-dodecamer (1,2,4, 12) association. Mazer et al. [7] concluded that their quasielastic light scattering data on several conjugated bile salt solutions in 0.15 and 0.60 M NaCl could be described as a monomer in equilibrium with a small 'primary micelle' which underwent a stepwise association to larger aggregates. If the so-called primary micelle is a dimer, then this is in accord with the type IV SEK model. The primary micelle could have a low value, since Mazer et al. [7] reported an average aggregation number 3 ± 1 for sodium taurocholate.

Whether the driving force for the self-association of bile salts is through hydrophobic interactions as advocated by Mazer et al. [7], or by hydrophobic bonding and then subsequent hydrogen bonding as proposed by others [2,3,6] remains to be seen. The Vadnere and Lindenbaum [6] model has the charged carboxylate ions at maximum separation, and their model indicates that trimer would be less stable electrostatically compared to tetramer. This is in accord with our type IV SEK model for sodium cholate, since in this association all odd species beyond trimer are absent (see the appendix). While this model involves several simultaneous equilibria, only two equilibrium constants are required (see the appendix). It would be possible to have significant amounts of association due to both hydrophobic and hydrogen bonding interactions with the type IV SEK

model even at relatively low concentrations of a few grams per liter.

Acknowledgements

This work was supported by grants from the National Institute of General Medical Sciences (GM 23877) and the Robert A. Welch Foundation (A485). J.M.B was a Robert A. Welch Foundation Fellow.

Appendix

The type IV SEK indefinite self-association can be described by a series of simultaneous equilibria

$$\begin{aligned} &P_1 + P_1 \leftrightharpoons P_2 \quad [P_2] = K_{12}[P_1]^2 \\ &P_2 + P_2 \leftrightharpoons P_4 \quad [P_4] = K_{12}^2 K_{24}[P_1]^4 \\ &P_2 + P_4 \leftrightharpoons P_6 \quad [P_6] = K_{12}^3 K_{24} K_{46}[P_1]^6 \\ &\text{etc.} \qquad\qquad \text{etc.} \end{aligned} \tag{A1}$$

If we assume that $K_{24} = K_{46} = \ldots = K$, then

$$\begin{aligned} &[P_2] = K_{12}[P_1]^2 \\ &[P_4] = K_{12}^2 K [P_1]^4 \\ &[P_6] = K_{12}^3 K^2 [P_1]^6 \\ &\qquad \text{etc.} \end{aligned} \tag{A2}$$

Now convert from molar concentrations to concentrations in g/l; thus

$$[P_i] = c_i/M_i = c_i/(iM_1) \tag{A3}$$

This leads to

$$\begin{aligned} c &= c_1 + 2k_{12}c_1^2 + 4k_{12}^2 k c_1^4 + 6k_{12}^3 k^2 c_1^6 + \ldots \\ &= c_1\left(1 + \frac{2k_{12}c_1}{[1 - k_{12}kc_1^2]^2}\right) \\ &= c_1\left(1 + \frac{2y}{[1 - z^2]^2}\right), \qquad \text{if } z < 1 \end{aligned} \tag{A4}$$

Here

$$k_{12} = K_{12}/M_1 \tag{A5}$$

$$k = K/M_1 \tag{A6}$$

$$y = k_{12}c_1 \tag{A7}$$

$$z^2 = k_{12}kc_1^2 \tag{A8}$$

The equations for f_1, M_1/M_{nc} and M_1/M_{wc} are

$$f_1 = 1/\left(1 + \frac{2y}{[1 - z^2]^2}\right) \tag{A9}$$

$$M_1/M_{nc} = \frac{1 + [y/(1 - z^2)]}{1 + [2y/(1 - z^2)^2]} \tag{A10}$$

and

$$M_1/M_{wc} = \frac{1 + [2y/(1 - z^2)^2]}{1 + [4y(1 + z^2)/(1 - z^2)^3]} \tag{A11}$$

The analysis is carried out as described by Beckerdite et al. [36].

References

1 T.M. Devlin, Textbook of biochemistry with clinical correlations (John Wiley and Sons, New York, 1982).
2 M.C. Carey and D.M. Small, Arch. Int. Med. 130 (1972) 506.
3 D.M. Small, in: The bile acids, eds. P.P. Nair and D. Kritchevsky (Plenum Press, New York, 1971) vol. 1, p. 249.
4 Y. Chang and J.R. Cardinal, J. Pharm. Sci. 67 (1978) 174, 994.
5 J.R. Cardinal, Y. Chang and D.D. Ivanson, J. Pharm. Sci. 67 (1978) 854.
6 M. Vadnere and S. Lindenbaum, J. Pharm. Sci. 71 (1982) 875.
7 N.A. Mazer, M.C. Carey, R.F. Kwasnick and G.B Benedek, Biochemistry 18 (1979) 3064.
8 D.M. Small, Adv. Chem. Ser. 84 (1968) 31.
9 W.S. Bennet, G. Eglinton and S. Kovac, Nature 214 (1976) 776.
10 D.G. Oakenfull and L.R. Fisher, J. Phys. Chem. 81 (1977) 1838.
11 R. Zana, J. Phys. Chem. 82 (1978) 2440.
12 D.M. Small, S.A. Penkett and D. Chapman, Biochim. Biophys. Acta 176 (1969) 178.
13 P. Ekwall, Int. Colloq. Biochem. Probl. Lipiden, Brussels 1953 (Brussels, 1954) p. 104.
14 P. Ekwall, J. Colloid Sci. 9, Suppl. 1 (1954) 66.
15 P. Ekwall, K. Fontell and A. Norman, Acta Chem. Scand. 11 (1957) 190.
16 P. Ekwall, K. Fontell and A. Stern, 2nd Int. Congr. Surface Activity, (London 1957) vol. 1, p. 357.
17 P. Ekwall, 4th Int. Congr. Surface Active Substances, Brussels 1964 (Gordon and Breach, New York, 1967) vol. 2, p. 651.

18 K. Fontell, Kolloid Z. Z. Polym. 241 (1971) 246.
19 K. Fontell, Kolloid Z. Z. Polym. 244 (1971) 253.
20 K. Fontell, Kolloid Z. Z. Polym. 250 (1972) 333.
21 M.C. Carey and D.M. Small, J. Colloid Interface Sci. 59 (1969) 382.
22 J.P. Kratohvil and H.T. DelliColli, Can. J. Biochem. 46 (1968) 945.
23 J.P. Kratohvil and H.T. DelliColli, Fed. Proc. 20 (1970) 1335.
24 P. Eneroth, J. Lipid Res. 4 (1963) 11.
25 V.H. Gänshirt, F.W. Koss and K. Morianz, Arzneim.-Forsch. 10 (1963) 943.
26 E.T. Adams, Jr, P.J. Wan and E.F. Crawford, Methods Enzymol. 48 (1978) 69.
27 B.W. Foster, J. Robeson, N. Tagata, J.M. Beckerdite, R.L. Huggins and E.T. Adams, Jr, J. Phys. Chem. 85 (1981) 3715.
28 J. Robeson, B.W. Foster, S.N. Rosenthal, E.T. Adams, Jr and E.J. Fendler, J. Phys. Chem. 85 (1981) 1254.
29 J. Visser, R.C. Deonier, E.T. Adams, Jr and J.W. Williams, Biochemistry 11 (1972) 2634.
30 L.-H. Tang and E.T. Adams, Jr, Arch. Biochem. Biophys. 157 (1973) 520.
31 W.E. Ferguson, C.M. Smith, E.T. Adams, Jr and G.H. Barlow, Biophys. Chem. 1 (1975) 325.
32 K.E. van Holde and R.L. Baldwin, J. Phys. Chem. 62 (1958) 734.
33 J.L. Sarquis and E.T. Adams, Jr, Biophys. Chem. 4 (1976) 81.
34 E.T. Adams, Jr, L.-H. Tang, J.L. Sarquis, G.H. Barlow and W.M. Norman, in: Physical aspects of protein interactions, ed. N. Catsimpoolas (Elsevier-North Holland, New York, 1978) p. 1.
35 L.-H. Tang, D.R. Powell, B.M. Escott and E.T. Adams, Jr, Biophys. Chem. 7 (1977) 121.
36 J.M. Beckerdite, C.C. Wan and E.T. Adams, Jr, Biophys. Chem. 12 (1980) 199.
37 E.T. Adams, Jr and H. Fujita in: Ultracentrifugal analysis in theory and experiment, ed. J.W. Williams (Academic Press, New York, 1962) p. 249.
38 N.E. White and M. Kilpatrick, J. Phys. Chem. 59 (1955) 1044.
39 A.V. Tobolsky and R.E. Thach, J. Colloid Sci. 17 (1962) 49.
40 G.A.D. Haselwood in: Bile salts, eds. R. Peters and F.G. Young (Methuen, London, 1967) p. 59.
41 A Vrij and J.T.G. Overbeek, J. Colloid Sci. 17 (1962) 570.
42 E.F. Casassa and H. Eisenberg, Adv. Protein Chem. 19 (1964) 287.
43 P. Carpenter and S. Lindenbaum, J. Solution Chem. 8 (1979) 347.
44 T.C. Laurent and H. Persson, Biochim. Biophys. Acta 106 (1965) 616.
45 E. Reisler and H. Eisenberg, Biochemistry 11 (1969) 4572.
46 T. Arakawa and S.N. Timasheff, Biochemistry 21 (1982) 6545.
47 C. Edelstein and A.M. Scanu, J. Biol. Chem. 225 (1980) 5747.
48 H.S. Harned and B.B. Owen, The physical chemistry of electrolytes, 2nd edn. (Reinhold, New York, 1950) p. 250.
49 R. Zana, J. Lang, S.H. Yiv, A. Djavanbakt and C. Abad in: Micellization, solubilization and microemulsion, ed. K.L. Mittal (Plenum Press, New York, 1977) vol. 1, p. 291.
50 P. Ekwall, Acta Acad. Aboensis, Math. Phys. 17 (1951) 8.
51 K. Fontell, Kolloid Z.Z. Polym. 246 (1971) 614, 710.
52 P. Debye, J. Phys. Colloid Chem. 51 (1947) 18.
53 P. Debye, J. Phys. Colloid Chem. 53 (1949) 1.
54 P. Debye, Ann. N. Y. Acad. Sci. 51 (1949) 575.
55 C.J. Biaselle and D.B. Millar, Biophys. Chem. 3 (1975) 355.